Effects of tree characteristics and sediment condition on critical breaking moment of trees due to heavy flooding

Norio TANAKA[*, 1)] and Junji YAGISAWA[*]

*Graduate School of Science and Engineering, Saitama University, Japan

[1)] 255 Shimo-Okubo, Sakura-ku, Saitama-shi, Saitama-ken 338-8570, Japan

tel/fax: +81-48-858-3564

e-mail: tanaka01@mail.saitama-u.ac.jp

Abstract

To elucidate tree breakage conditions with different breaking mechanisms, i.e., moment by drag force, local scour, and degradation of the substrate around trees, field surveys were conducted after a flood event (September 2007 flood due to Typhoon 9) in the Tamagawa River, Japan. Trees in a river have two main breaking mechanism at a flood event, moment by fluid force and erosion of the substrate. Moment by fluid force causes two breaking phenomena, trunk damage (bending, breakage) and overturning. Trunk bending or breakage can be expressed by the function of d^c, where d is the trunk diameter at breast height, the power c equals 3 in the trunk bending or breakage, and around 2 in overturning. Smaller diameter trees received trunk breakage, but larger trees were overturned. The range for these two breaking patterns changes with the substrate condition. If severe scouring has occurred, the threshold overturning moment

can be quite small. Tree overturning occurred mostly on the bank side of the gravel bar; however, some trees, especially *Robinia pseudo-acacia* and *Morus bombycis*, were overturned if the substrate was a thin deposited soil or silt layer on gravel. The roots were anchored in the small particle deposited layer in that case. As for the erosion of the substrate, the tree breaking patterns can be classified into three types depending on the relationship between the non-dimensionalized bed shear stress of d_{50} and d_{84}, the representative grain diameters at which 50% and 84% of the volume of small particles, respectively. The non-dimensionalized shear stress of d_{84} is an important parameter for discussing the rehabilitation of the gravel bed bar. The boundary region for tree overturning can be changed by the effects of plant cover and debris attachment.

Key words: tree breaking pattern, forestation, regeneration, root zone, moment by drag force

Introduction

Vegetation in rivers creates a valuable natural environment that maintains the biodiversity. However, vegetation affects channel morphologies by increasing local roughness (Kouwen and Fathi-Morgan, 2000), creating obstructions to flow (Wallerstein and Thorne, 2004), providing sedimentation sites (Wyzga, 2001), and strengthening the bank against lateral channel erosion (Graf, 1978; Pollen, 2007). The forestation in a river sometimes becomes a problem not only because it reduces river flow capacity to the downstream, but because the debris, i.e., broken tree-trunks and branches, increase drag force on bridge piers in rivers and cause a larger scour hole than would occur without vegetation when the floating debris are attached to and accumulate around the pier (Melville and Dongol, 1992). In addition, the excessive forestation by a single species of tree or invasive exotic tree species sometimes affects the biodiversity in a

river habitat (Maekawa and Nakagoshi, 1997). Rehabilitation of a gravel bed river and removal of trees have been discussed recently (Oswalt and King, 2005).

Considering the above situation, elucidation of the breaking conditions of river vegetation by floods is necessary. The breaking condition of trees due to wind damage (Gardiner et al., 2000) can be classified and estimated by the moment (=(drag force acting on tree) ×(length from the trunk base to the acting point)) acting on the forest trees. The breaking mechanism of a tree in a river is similar to that of wind damage, but quantification is very difficult because the relationship between tree height and water depth changes in the cases of river floods or tsunamis (Tanaka et al., 2006, 2007). Like the flow pattern around a circular cylinder (Okamoto and Sunabashiri, 1992; Baker, 1980), the change in water depth is assumed to affect the flow pattern around a tree and the drag force (Kouwen and Fathi-Morgan, 2000). An increase in drag force is assumed to decrease the average shear stress on the substrate around a tree, considering shear stress partitioning (Einstein, 1950). Then the flow structure and breaking pattern of river vegetation due to a flood become more complex.

Therefore, the objectives of this study are to 1) investigate the breaking pattern of trees in a river due to floods, 2) elucidate quantitatively the critical turning or breaking moment needed to uproot or break tree trunks, and 3) propose a method for estimation of the amount of tree breaking considering the moment and bed shear stress. For these objectives, the damage to trees in a river on gravel bars or on floodplains after a flood event was investigated in detail.

Analysis and Field Survey

Analysis of tree-breaking threshold considering different breaking mechanisms

Definition of breaking pattern and critical breaking moment

The tree breaking pattern was classified into four patterns in this study (Fig. 1), although it can

be classified mainly by two mechanisms: 1) trunk bending or breakage and 2) overturning or uprooting. Trunk bending or breakage occurs when the maximum shear stress by the bending moment at the tree trunk section exceeds the critical shear stress for elastic bending in each tree. When the shear stress exceeds the threshold value for elastic bending deformation, plastic bending (PB) deformation starts. If the deformation is within the plastic bending range, we can define it as 'bending damage', but when the stress exceeds the plastic bending range, trunk breakage (TB) occurs (Fig. 1a). Overturning or uprooting occurs when the maximum shear stress around the root anchoring zone due to the bending moment exceeds a critical value (Gardiner et al., 2000). Some trees are not overturned after the deformation starts because the shear stress is smaller than the sum of the root tensile strength or pullout forces (Tosi, 2007; Pollen, 2007), as shown in Fig. 1b (hereafter, called 'partial overturning' (POV)). If the shear stress is larger than the total resistance force by roots, the tree is completely overturned, as shown in Fig. 1c (hereafter, 'overturning' (OV)). In addition, even when breaking like shown in Fig. 1a, 1b, and 1c did not occur (hereafter, NOB), local scouring like that shown in Fig. 1d usually occurred.

Gardiner et al. (2000) proposed two equations for tree breaking thresholds, trunk breakage and overturn. The trunk breakage moment, M_{bc} (kNm), can be calculated as:

$$M_{bc} = \frac{\sigma_{\max} I}{R} \cong kd^3 \tag{1}$$

where R and d are the radius and diameter, respectively, of the breaking section of a tree trunk (m), $\sigma_{\max}$ is the critical bending moment of the outer fiber of the tree trunk (N/m^2), and I is the second moment of area (m^4). If $\sigma_{\max}$ is assumed to be constant, the breakage condition becomes a function of d^3. In that case, k becomes a constant dependent on the tree species.

The critical bending moment for overturning trees, M_{overc}, is proposed as a function of trunk weight (Gardiner et al., 2000) based on tree pulling experiments on almost 2000 trees as:

$$M_{overc} = k_{over} \times (trunk\ \ weight) \tag{2}$$

where k_{over} is a constant.

A similar equation was proposed by the Technology Research Center for Riverfront Development (TRCRD) (1994) as:

$$M_{turnc} = 24.5 d_{BH}{}^2 \tag{3}$$

where M_{turnc} is the critical overturning moment of a tree in rivers (Nm), and d_{BH} is the diameter of a tree trunk at breast height (cm). This corresponds to the assumption that the trunk weight is proportional to $d_{BH}{}^2$ in Eq. (2).

To investigate tree-specific characteristics for trunk breakage, a loading test for river trees was conducted in an experimental laboratory at Saitama University (Fig. 2). Six *Salix subfragilis* (diameter of tested-tree pieces, d_T = 2.7–10.7 cm) and 6 *Robinia pseudo-acacia* (d_T = 2.6–12.0 cm) trees were used. With these experiments, the constant k in Eq. (1) was estimated for each species.

One more important mechanism for resisting bending moment is root tensile strength. As roots increase soil shear strength by anchoring in a soil layer and by forming a binding network (Tosi, 2007), they increase the threshold moment for overturning when soil shear stress exceeds the critical value of soil shear strength. This will be discussed in the Results.

Analysis of moment acting on tree trunk

To analyze the moment acting on a tree, M, we considered the drag force, F, including the tree stand structure (Tanaka et al., 2007) as:

$$\begin{aligned} F &= \int_0^h \frac{1}{2} C_d(z) \rho u(z)^2 d(z) dz = \frac{1}{2} \rho C_{d-ref} D_{BH} U^2 \int_0^h \frac{d(z)}{D_{BH}} \frac{C_d(z)}{C_{d-ref}} dz \\ &= \frac{1}{2} \rho C_{d-ref} D_{BH} U^2 \int_0^h \alpha(z) \beta(z) dz \end{aligned} \tag{4}$$

$$\alpha(z) = \frac{d(z)}{D_{BH}} \quad , \quad \beta(z) = \frac{C_d(z)}{C_{d-ref}} \tag{5}$$

$$M = \frac{1}{2} \rho C_{d-ref} D_{BH} U^2 \int_0^h z \alpha(z) \beta(z) dz \tag{6}$$

where z (m) = vertical axis from the bottom, $C_{d\text{-}ref}$, reference drag coefficient (=1 considering a circular cylinder in this study), $C_d(z)$, $u(z)$, $d(z)$ = drag coefficient, velocity(m/s), cumulative width of tree trunks and branches (m) at height z, respectively, ρ (kg/m^3) = density of fluid, h (m) = flood water depth, D_{BH} (m) = breast height diameter of a tree trunk (=0.01d_{BH} (cm); we distinguish d_{BH} and D_{BH} in this study), $\alpha(z)$ = additional coefficient expressing the vertical tree structure, and $\beta(z)$ = additional coefficient representing the effect of leaves and the inclination of branches. For the value of $\beta(z)$, previous research indicated that the additional drag by leaves themselves can be assumed to be a constant value (1.25 (Fukuoka and Fujita, 1990) and 1.4 (Armanini et al., 2005)). Because the sensitivity of this parameter is not very large in considering the breaking condition, we used 1.25 for $\beta(z)$ considering that the effects of the inclination of branches were assumed to be larger than those in the condition of Armanini et al. (2005). In this research, the vertical velocity distribution was not considered, and the sectional average velocity U (m/s) was used for $u(z)$(Fig. 3). For determining the downward limit of threshold breaking moment, M was calculated using the estimated velocity (U) at the maximum water depth (h), and comparing the moment on broken trees with not broken trees after the flood event. For more details, see Tanaka et al. (2007).

Critical shear stress estimation for d_{50} and d_{84}

To evaluate the shear stress acting on the grain, τ_{*i}, the non-dimensionalized shield parameters that are usually used for considering 'the gravity force (slope direction)' over 'the weight of the grain in water' were used as below:

$$\tau_{*i} = \frac{\rho g H I_b}{(\rho_s - \rho) g d_i} = \frac{H I_b}{\left(\frac{\rho_s}{\rho} - 1\right) d_i} \tag{7}$$

where ρ_s and ρ is the density of the particles and water, respectively, g is the gravitational acceleration, d_i is the grain diameter at which i % volume passed through the sieve, and I_b is the

bed slope.

The critical shear stress of d_{50} for the initiation of motion, τ_{*c50} can be approximated from the Shields diagram (i.e., Graf (1984)) as:

$$\frac{\tau_{*c50}}{(\rho_s - \rho)gd_{50}} = 0.06 \tag{8}$$

To calculate the effects of the grain size distribution, the critical shear stress of each grain size i, τ_{*ci}, as proposed by Egiazaroff (1965), was:

$$\frac{\tau_{*ci}}{(\rho_s - \rho)gd_i} = \frac{0.1}{\left[\log_{10} 19(d_i / d_m)\right]^2} \tag{9}$$

where, d_m is the medium grain size.

τ_{*50}, τ_{*84} is derived by substituting $d_i = d_{50}$ or d_{84} in Eq. (7), respectively.

τ_{*c84} is derived by substituting $d_i = d_{84}$ in Eq. (9).

The reasons that d_{84} was selected for classifying tree breaking pattern including the bed degradation mechanism were 1) the maximum grain diameter, d_{max} and d_{84} are dominant parameters for expressing the bedload transport (Blizard and Wohl (1998)), 2) d_{max} is difficult to be decided from the sample (sample error is large), 3) d_{84} is related to the geometric standard deviation, $\sigma_g = d_{84}/d_{50}$, when the sediment profile in the river can be expressed in logarithmic normal distribution (Otto, 1939), and 4) local scour depth around a bridge pier (similar to tree trunk) including the armouring phenomena are closely related to d_{84} and d_{50} (Melville and Sutherland, 1988).

Field investigation

Field investigations were conducted at Todoroki (TO), Komae (KO), Inagi (IN), Fuchuyotsuya (F1 and F2), Hinobashi (HI), Mutsumebashi (MU), and Nagatabashi (N1 and N2) in the Tamagawa River (Fig. 1(a)), Japan, after Typhoon 9 in September, 2007. The

characteristics of each location are listed in Table 1. Breaking patterns of trees and flood water marks were investigated at each site. The maximum water depths around trees were measured by the height at which debris was attached or branches were broken. The photographs in Fig. 1(b) show the tree breaking pattern at representative sites. At each site, the debris attached to tree trunks was observed, as in photo KO. In addition, large scour holes like those shown in photo F1 were caused by three dimensional eddies, mainly horse-shoe vortices like those around a pier (Raudkivi and Ettema, 1983) and Kármán type eddies in the wake (Takemura and Tanaka, 2007). Tree-breaking patterns were assumed to be related to the substrate condition because some trees were uprooted and the substrate was completely washed away (see photo N2), but some trees remained standing when the substrate was covered with vegetation (photo IN). From the observation, the tree characteristics (d_{BH}: tree trunk diameter at breast height), debris attachment width and height, maximum scour hole depth (h_s), and substrate condition (d_{50}, d_{84}: diameters at which 50% and 84% of the volume, respectively, are passed through a sieve) were selected for measurement.

Estimation of local velocity approaching trees

Two methods were used to estimate the flow velocity approaching trees.

Method 1

Most of the perennial grasses, i.e., *Miscanthus sacchariflorus*, in the investigated site were broken around the trees after the 2007 flood, but some remained standing. Tanaka et al. (2004) investigated the breaking moments of the perennial grasses *Phragmites australis* and *Miscanthus sacchariflorus* in a river habitat, and found them to be 0.62 Nm and 1.25 Nm, respectively, for 3-4 mm diameter stems. If the grasses are broken, the moment can be assumed larger than the critical value. From this we can assume the minimum velocity at the habitat. In the wake of a tree, *M. sacchariflorus* were sometimes not broken (Fig. 5). From Takemura and

Tanaka (2007), the wake flow velocity, u_{wake}, can be assumed as:

$$u_{wake} = \gamma U \tag{10}$$

where U is the approaching velocity to colony-type trees, and γ is a constant depending on G/D, where G is a cross-stream gap between trees and D is a reference diameter of the trees. From field investigations, $G/D = 1$ and 2 for *Robinia pseudo-acacia* and *Salix subfragilis*, respectively, and they correspond to $\gamma = 0.70$ and 0.65, respectively. When *M. sacchariflorus* was not broken, we can assume the maximum value of u_{wake} from the threshold breaking moment of the plant. From u_{wake}, the maximum value of U can be assumed.

Method 2

The water surface gradient from Hinobashi Station to Chofubashi Station, which are located upstream and downstream of Hinobashi (HI), Mutsumebashi (MU), and Nagatabashi (N1 and N2), was about 1/240. This value is similar to the bed gradients, 1/290, 1/228, and 1/228 for HI, MU, and N1(N2), respectively. Thus, quasi-normal flow was assumed to evaluate the velocity at the damaged trees on the gravel bar. This method can be applied to a flood peak event when the water surface gradient and bed gradient are not very different from each other. The Manning equation and Manning roughness coefficient, n_w, which includes surface roughness and resistance by grasses (Petryk and Bosmajian, 1975) are used to evaluate the flow velocity in each habitat. The coefficient is given as:

$$n_w = \sqrt{{n_b}^2 + \frac{C_d}{2g} a_w {h_w}^{\frac{4}{3}}} \tag{11}$$

where n_b = surface roughness ($m^{-1/3}s$), a_w = projected area of plants in unit volume (m^2/m^3), and h_w = vegetation height (m).

Results

Breaking condition of tree trunks

The velocities calculated from Method 1 were 1.52-2.17 m/s for Nagatabashi. The values were similar to the values estimated by Method 2, 1.10 - 2.53 m/s for Nagatabashi. Thus, we estimated the velocity by Method 1 if we had data available for Method 1. Otherwise, the velocity values estimated by Method 2 were used for calculating the moment at the flood event.

Fig. 6a shows one example of the relationship between the displacement and the loading force at the loading test. When the force reaches the critical force for yield, the gradient of 'Loading force/displacement' becomes small. Thus, we define the force as 'yield force,' and this is the limitation of elastic bending. When the deformation becomes large, the outer fiber of the tested-tree pieces is broken. Then, we define the force as the force for trunk breakage. By using the force and arm length, the plastic bending (PB) moment and trunk breakage (TB) moment can be estimated. Figures 6b and c show the relationship between the trunk diameters and the breaking moments for the representative tree vegetations, *Salix subfragilis* and *Robinia pseudo-acacia*, respectively. The k in Eq. (1) is evaluated as 3 for *S. subfragilis* and 2 for *R. pseudo-acacia* by the loading test of the tree trunk (Fig. 2). The threshold trunk breakage moment of *R. pseudo-acacia* is smaller than that of *S. subfragilis*, because the bending stiffness (EI) of the *R. pseudo-acacia* trunk is smaller and more easily broken than the trunk of *S. subfragilis*.

Fig. 7 a and b show the relationship between d_{BH} and moment by drag force (M) acting on *S. subfragilis* and *R. pseudo-acacia* at the Typhoon 9 flood event. Dotted lines in Fig. 7 show the threshold moments for trunk breakage estimated in Fig. 6, and these figures also validate the curves in Fig. 6b and c, respectively. The trend in the flood event data shows that the M_{bc} has a

function of d_{BH} cubed, as indicated in Eq. (1).

Overturning moment of river vegetation

Paying attention to the overturning (OV) phenomena at the flood event, the relationship between the trunk diameter at breast height and the moment due to drag force acting on the trunk base were calculated (Fig. 8). This figure distinguishes the data on whether the tree is broken or not and whether the tree-anchoring substrate is a gravel layer (GL) or a deposited layer (DL). If the tree, in this case *R. pseudo-acacia* (at IN) or *Morus bombycis* (at N2), is growing on a floodplain consisting of sand and silt and the root is restricted to this zone, the threshold moment for overturning is low compared with the curve in Eq. (3). However, if the tree, in this case *Salix* spp. (at HI), is growing on a gravel bar and the roots are anchored in the substrate, the threshold moment for overturning is relatively larger than the value in Eq. (3).

To evaluate the substrate effect clearly, the relationships between the non-dimensionalized shear stresses of d_{50} and d_{84} and the breaking pattern of trees were investigated (Fig. 9). Fig. 9a shows a schematic diagram of scouring situation around trees classified by τ_{*50}/τ_{*c50} and τ_{*84}/τ_{*c84}. In Fig. 9a, the graph area can be devided into three groups; Region A, Region B and Region C. In Region A, the scouring phenomenon is a ‘quasi-clear water scour’. ‘Quasi-clear water scour’ is defined in this study as the local scour phenomenon around a tree when d_{50} outside of the local scour region is not moved that is similar to the ‘clear water scour’ under uniform diameter grain (Raudkivi and Ettema, 1983). In Region B, the scouring phenomenon is changed to a scour with sediment transport (hereafter, live-bed scour (Raudkivi and Ettema, 1983)). In this region, d_{50} can be moved but d_{84} cannot be moved. It is difficult to wash out trees in this region because the grains with diameter larger than d_{84} are difficult to be moved and the armoring is occurred. In Region C, the scouring phenomenon can be classified as a live-bed scour where most of gravel is assumed to be moved

easily. It is possible to wash out trees in this region.

If the tree is anchored in the gravel layer, the threshold shear stress is closely related to d_{84}. However, if the root zone is restricted to the deposited layer on the gravel bar, like some trees in N2, FU and IN, the threshold drag moment by drag force is quite small, as shown in Fig. 8. The τ_{*84} / τ_{*c84} values of the three habitats are very large. This indicates that the removal condition is controlled not only by the moment but also by the substrate condition. To analyze the substrate effect, the parameter τ_{*84} / τ_{*c84} is better for expressing the tree overturning. On the other hand, when τ_{*84} / τ_{*c84} is around 1, both overturning and partial overturning occurred and are not clearly distinguished. If perennial grasses are growing around a tree like Inagi (IN), as shown in Fig. 4 (Photo-IN), the threshold becomes large, as indicated by Parsons (1963).

Discussion

Change of breaking pattern and its threshold breaking moment

In the case of the river flood investigated here, trunk breakage seldom occurs during the flood, but the bending pattern does. The locations at which the tree overturning occurred are restricted to the bank side of the gravel bar or the flood plain that had a thin deposited layer (DL) of silt or sand on a gravel bed bar. In those cases, the sediment grain size around the tree is not large. Most *Salix* spp. are not overturned, but *R. pseudo-acacia* and *M. bombycis* on DL are. This indicates that the timing of the colonization of the tree species is also an important factor. The deposition decreases the tree overturning moment, however, if the DL is covered with a perennial grass such as *M. sacchariflorus*, which has strong soil binding network of rhizome and roots, and increases the threshold of the tree overturning. Tree overturning can be assumed to be strongly affected by the substrate condition. On the other hand, the results shown in Fig. 7 indicate that the trunk breakage depended on the tree-trunk material, but the tree overturning

threshold in Fig. 8 could be changed by the substrate condition, as shown in the schematic in Fig. 10a. In addition, at the crossing point of the two equations for bending and overturning damage, the trunk diameter is important for understanding the tree damage mechanism.

Effect of substrate condition and perennial plant cover on renewal of gravel bar

The threshold moment may be expressed as a function of the substrate condition. Compared with wind damage (Gardiner et al., 2000) or tsunami damage (Tanaka et al., 2007), the scouring effect is sometimes more severe in the case of a river flood. Thus, in addition to the moment acting on the tree, the shear stress condition should be discussed in this section. Fig. 10b shows the schematic diagram of Fig. 9b that expresses the relationship between τ_{*50}/τ_{*c50} and τ_{*84}/τ_{*c84}. The graph area can be classified into three groups with the investigated river bed gradient which ranges from 1/228 to 1/729, and with the investigated ranges of d_{BH} plotted in the three regions, i.e., 17-54 cm (NOB) and 3-22 cm (PB) in Region A, 18cm (NOB), 7-9cm (PB) and 5-18cm (POV) in Region B, and 7-22cm (POV) and 13-40cm (OV) in Region C. In Region A, the scouring phenomenon is a quasi-clear water scour and the tree breaking pattern is mainly bending damage (PB and TB). If the moment is not large enough to overturn the tree, even if debris are attached, then the scouring does not much affect the threshold for overturning in this region. In Region B, the scouring phenomenon is changed to a live-bed scour and the tree breaking pattern is mainly partial overturning or overturning when τ_{*84}/τ_{*c84} is about 1. In this region, an armoring phenomenon (Breusers et al., 1977) occurs, because the gravels with diameter larger than d_{84} are not moved. In Region C, the scouring phenomenon is a live-bed scour and most of the gravel can be moved easily. Then, if τ_{*84}/τ_{*c84} is much larger than 1, trees are easily overturned and sometimes even washed out when the moment is small (Fig. 8). However, unless the water depth is higher than the tree crown height, most of the debris are attached to trunks near the bed and the additional moment by drag is not large. When τ_{*84}/τ_{*c84}

is a little smaller than one, the additional moment becomes larger because the water depth increases. As shown in Fig. 8, plant cover on the substrate also affects the tree breakage condition when τ_{*84}/τ_{*c84} is a little larger than one. Therefore, the plant cover and debris attachment affects the tree overturn threshold mainly when τ_{*84}/τ_{*c84} is around one, i.e., at the boundary of Region B and Region C (hereafter, 'boundary region'). From the point of view of rehabilitation of the gravel bed bar, flooding in Region C and in the boundary region is required. In contrast, the flooding in Region A does not much affect the vegetation, because the trees can easy regenerate from being bent and recover in the next year. However, because flooding in Region A sometimes accumulates much sediment in the vegetated area, the reforestation process after a flood in Region A requires more study in the future.

The range of riverbed gradient (I) is 1/228 to 1/729 in the Tamagawa River. If we apply this method to other rivers which have very mild slope and smaller gravel without our investigated range, the location of the breaking pattern (NOB, PB, TB, POV, OV) by moment in the schematic figure classified by non-dimensional shear stress by τ_{*50}/τ_{*c50} and τ_{*84}/τ_{*c84} as shown in Fig.10b will be changed. More study is needed to generalize this method for expressing the full mechanism of the tree breaking phenomena in rivers considering both the moment acting on trees and the bed shear stress.

Summary

A tree has two main breaking patterns related to moment by fluid force on the tree, trunk bending or breakage and overturning or uprooting (washing out). In terms of plant regeneration, trunk bending or breakage is not considered important. At this site, tree overturning and uprooting was restricted to the bank side of the gravel bar, but some trees, especially *Robinia pseudo-acacia* and *Morus bombycis*, were overturned if the substrate had a thin soil zone on the

gravel layer. The root zone was restricted in that case. The tree breaking patterns related to the erosion of the substrate can be classified into three patterns according to the relationship between τ_{*50}/τ_{*c50} and τ_{*84}/τ_{*c84}. τ_{*84}/τ_{*c84} is an important parameter for discussing the rehabilitation of the gravel bed bar. The boundary region for tree overturning can be changed by the effects of plant cover and debris attachment. The moment by drag force is an important parameter when we consider the bending and overturning damage in the boundary region in which τ_{*84}/τ_{*c84} is around one. This study elucidated the tree breaking phenomenon by considering the moment due to drag force and the substrate condition.

Acknowledgements

This study is partly funded by the Foundation of River & Watershed Environment Management (FOREM). Prof. Fukuoka, Chuo University, and Prof. Sasaki, Saitama University, are acknowledged for their useful suggestions. The authors would like to thank Mr. Nagai and Mr. Ito for their help in field measurements.

References

Armanini A, Righetti M, Grisenti P (2005) Direct measurement of vegetation resistance in prototype scale, Journal of Hydraulic Research **43**: 481-487.

Baker CJ (1980) The turbulent horseshoe vortex. J. Wind Engineering and Industrial Aerodynamics **6**: 9-23.

Blizard CR, Wohl EE (1998) Relationships between hydraulic variables and bedload transport in a subalpine channel, Colorado Rocky Mountains, U.S.A, Geomorphology **22**:359-371.

Breusers HNC, Nicollet G, Shen HW (1977) Local scour around cylindrical piers, J. Hydraulic Research **15**: 211-252.

Einstein HA (1950) The bed-load function for sediment transportation in open channel flows. USDA Technical Bulletin **1026**: 71.

Egiazaroff JV (1965) Calculation of Nonuniform sediment concentrations, Proc. Am. Soc. Civil Engineers **91(4)**: 225-247.

Fukuoka S, Fujita K (1990) Hydraulic effects of luxuriant vegetations on flood flow (in Japanese with English abstract), Report of PWRI **180(3)**: 64.

Gardiner B, Peltola H, Kellomäki S(2000) Comparison of two models for predicting the critical wind speeds required to damage coniferous trees, Ecological Modelling **129**: 1-23.

Graf WH (1984) Hydraulics of sediment transport, Water Resources Publications, LLC: 97.

Graf WL (1978) Fluvial adjustments to the spread of tamarisk in the Colorado Plateau region. Geological Society of America Bulletin **89**: 1491–1501.

Kouwen N, Fathi-Morgan M (2000) Friction factors for coniferous trees along rivers, J. Hydraulic Engineering **126(10)**: 732-740.

Maekawa M, Nakagoshi N (1997) Riparian landscape changes over a period of 46 years, on the Azusa River in Central Japan, Landscape and Urban Planning **37** : 37-43.

Melville BW, Dongol DM (1992) Bridge pier scour with debris accumulation, J. Hydraulic Engineering **118(9)**: 1306-1310.

Melville BW, Sutherland AJ (1988) Design method for local scour at bridge piers, J. Hydraulic Engineering **114(10)**: 1210-1226.

Okamoto S, Sunabashiri Y (1992) Vortex shedding from a circular cylinder of finite length placed on a ground plane, Transactions of the ASME. J. of Fluids Engineering **114**: 512-521.

Oswalt SN, King SL (2005) Channelization and floodplain forests: Impacts of accelerated sedimentation and valley plug formation on floodplain forests of the Middle Fork Forked Deer River, Tennessee, USA, Forest Ecology and Management **215**: 69–83.

Otto GH (1939) A modified logarighmic probability graph for the interpretation of mechanical

analyses of sediments, Journal of sedimentary petrology **9(2)**: 62-72.

Parsons DA (1963) Vegetative control of streambank erosion, Proc. Federal Interagency Sedimentation Conference, Miscellaneous Publication **970**, U.S. Department of Agriculture, Washington, D.C.: 130-136.

Petryk S, Bosmajian G.B (1975) Analysis of flow through vegetation. Journal of the Hydraulics Division, ASCE **101 (7)**: 871–884.

Pollen N (2007) Temporal and spatial variability in root reinforcement of streambanks: Accounting for soil shear strength and moisture, Catena **69**: 197–205.

Raudkivi AJ, Ettema R (1983) Clear-water scour at cylindrical piers, Journal of Hydraulic Engineering **109(3)**: 338-350.

Takemura T, Tanaka N (2007) Flow structures and drag characteristics of a colony-type emergent roughness model mounted on a flat plate in uniform flow, Fluid Dynamics Research **39**: 694–710.

Tanaka N, Kitakami Y, Ogawa T, Asaeda T (2004) Effect of stem-breaking caused by flood on the transition of wetland vegetation in old river trace, Proc. 4th ISEH/14th IAHR-APD: 1555-1562.

Tanaka N, Sasaki Y, Mowjood MIM (2006), Effects of sand dune and vegetation in the coastal area of Sri Lanka at the Indian Ocean tsunami, In: Eds, Namsik Park et al., Advances in Geosciences **6**, World Scientific Publishing, Co.

Tanaka N, Sasaki Y, Mowjood MIM, Jinadasa KBSN (2007), Coastal vegetation structures and their functions in tsunami protection: Experience of the recent Indian Ocean tsunami, Landscape and Ecological Engineering **3**: 33-45.

Technology Research Center for Riverfront Development (TRCRD) (1994), Guideline for tree management in rivers (in Japanese), Sankaidou: 154-160.

Tosi M (2007) Root tensile strength relationships and their slope stability implications of three shrub species in the Northern Apennines (Italy), Geomorphology **87**: 268–283.

Wallerstein NP, Thorne CR (2004) Influence of large woody debris on morphological evolution of incised, sand-bed channels, Geomorphology **57**: 53–73.

Wyzga, B (2001) Impact of the channelization-induced incision of the Skawa and Wisloka Rivers, southern Poland, on the conditions of overbank deposition, Regulated Rivers: Research & Management **17**: 85–100.

List of Figures

event. Breaking pattern was overturning. open symbol: not overturning (NOB), closed synmol: overturning (OV). Line and dotted lines show the threshold moment for overturning trees at gravel layer (GL) and deposited layer (DL), respectively.

Fig. 9 Relationship between non-dimensionalized shear stresses and the breaking pattern of trees. (a) definition of Region A, B and C considering the non-dimensionalized shear stresses τ_{*50}/τ_{*c50} and τ_{*84}/τ_{*c84} (Region A ; $\tau_{*50}/\tau_{*c50} < 1$ and $\tau_{*84}/\tau_{*c84} < 1$, Region B ; $\tau_{*50}/\tau_{*c50} > 1$ and $\tau_{*84}/\tau_{*c84} < 1$, Region C ; $\tau_{*50}/\tau_{*c50} > 1$ and $\tau_{*84}/\tau_{*c84} > 1$), (b) breaking pattern of trees plotted in the figure that expresses the relationship betweenτ_{*50}/τ_{*c50} and τ_{*84}/τ_{*c84}. For GL and DL, see the caption of Fig.8, For PB, POV, OV and NOB, see Fig. 1. open symbol : not overturning (NOB), closed symbol : overturning (OV).

Fig. 10 Schematic of change in threshold for tree breaking. (a) Moment by drag force, (b) non-dimensionalized shear stress

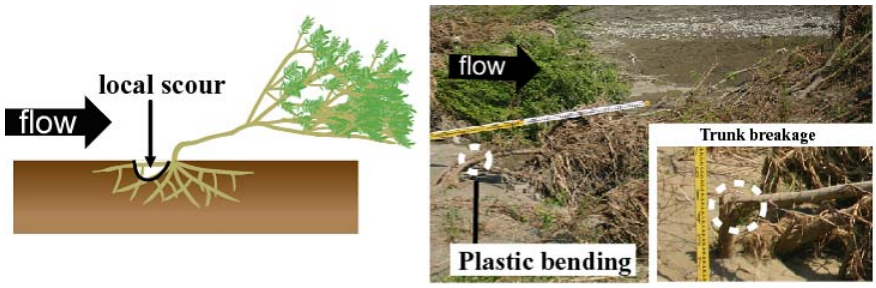

(a) Plastic bending (PB) and Trunk breakage (TB)

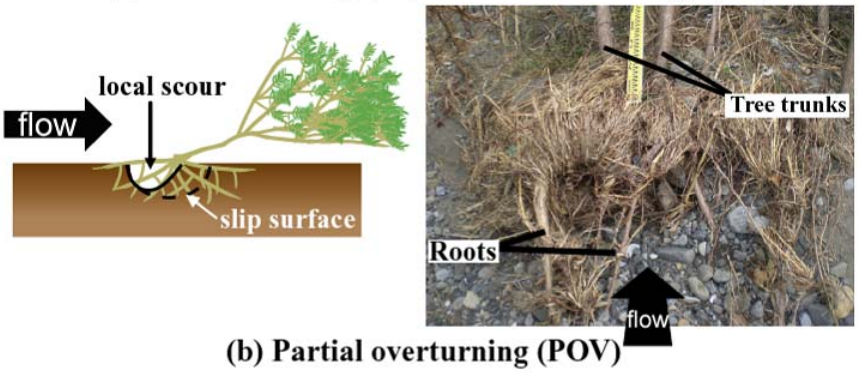

(b) Partial overturning (POV)

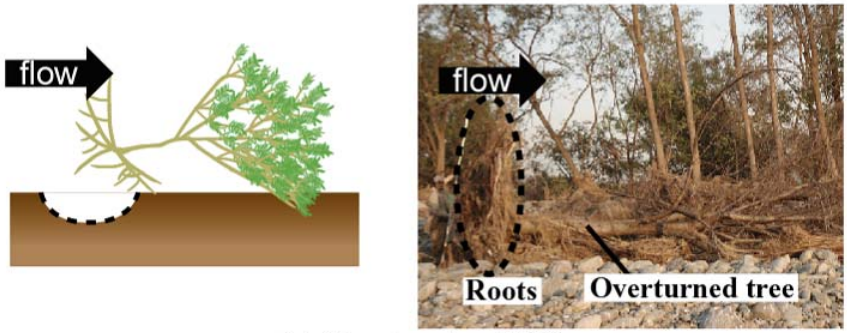

(c) Overturning (OV)

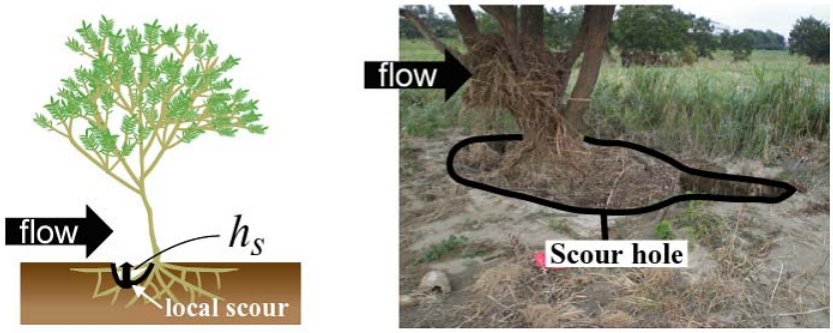

(d) Not overturning and bending but with local scour around a tree (NOB)

Fig. 1

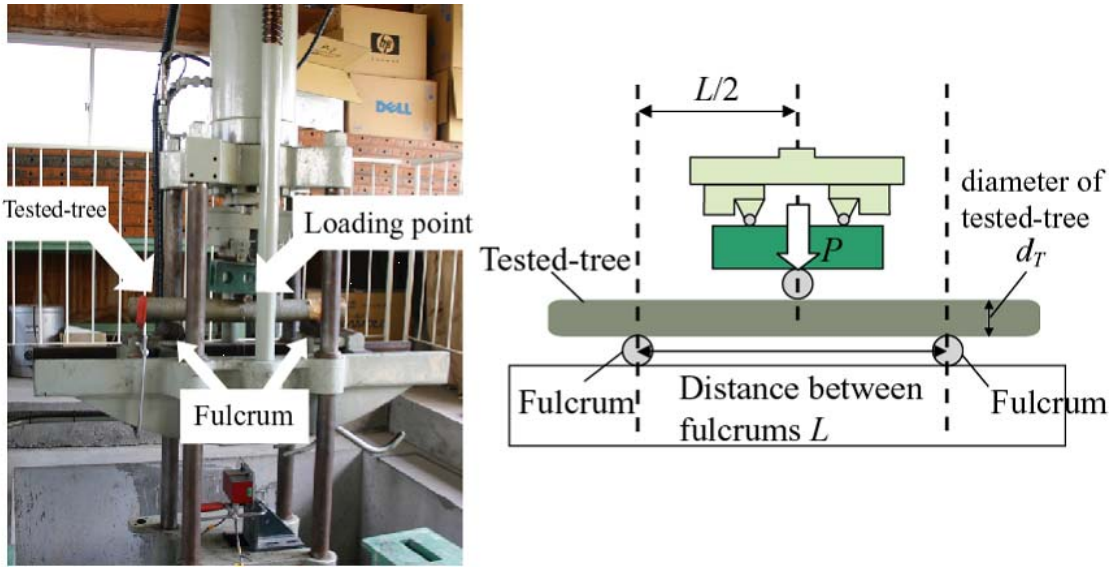
Tested-tree
Loading point
Fulcrum
L/2
diameter of
tested-tree
d_T
Tested-tree
P
Fulcrum
Distance between
fulcrums L
Fulcrum

Fig. 2

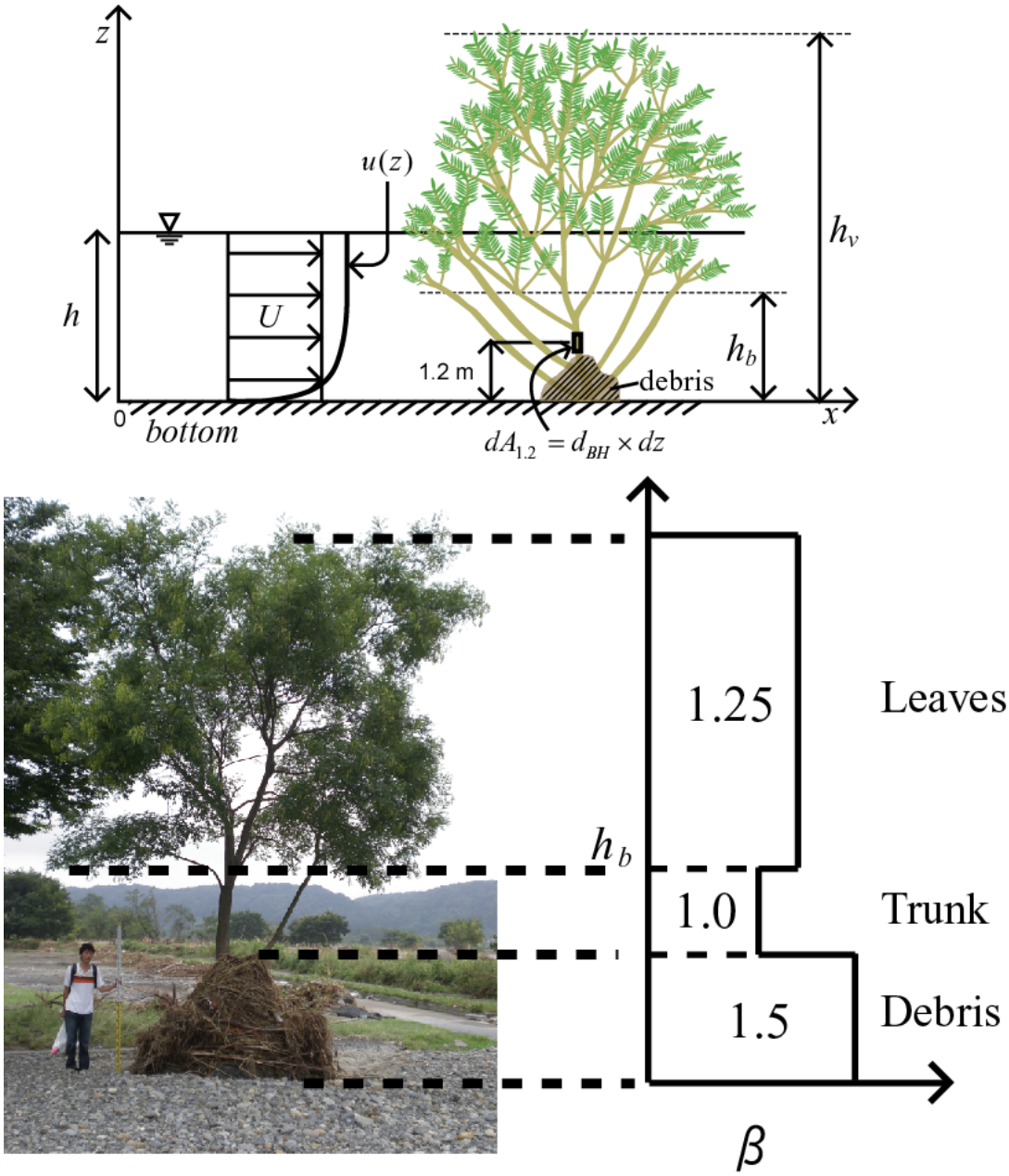
z
u(z)
h
U
h_v
h_b
1.2 m
debris
0
bottom
x
$dA_{1.2} = d_{BH} \times dz$
1.25
Leaves
h_b
1.0
Trunk
1.5
Debris
β

Fig. 3

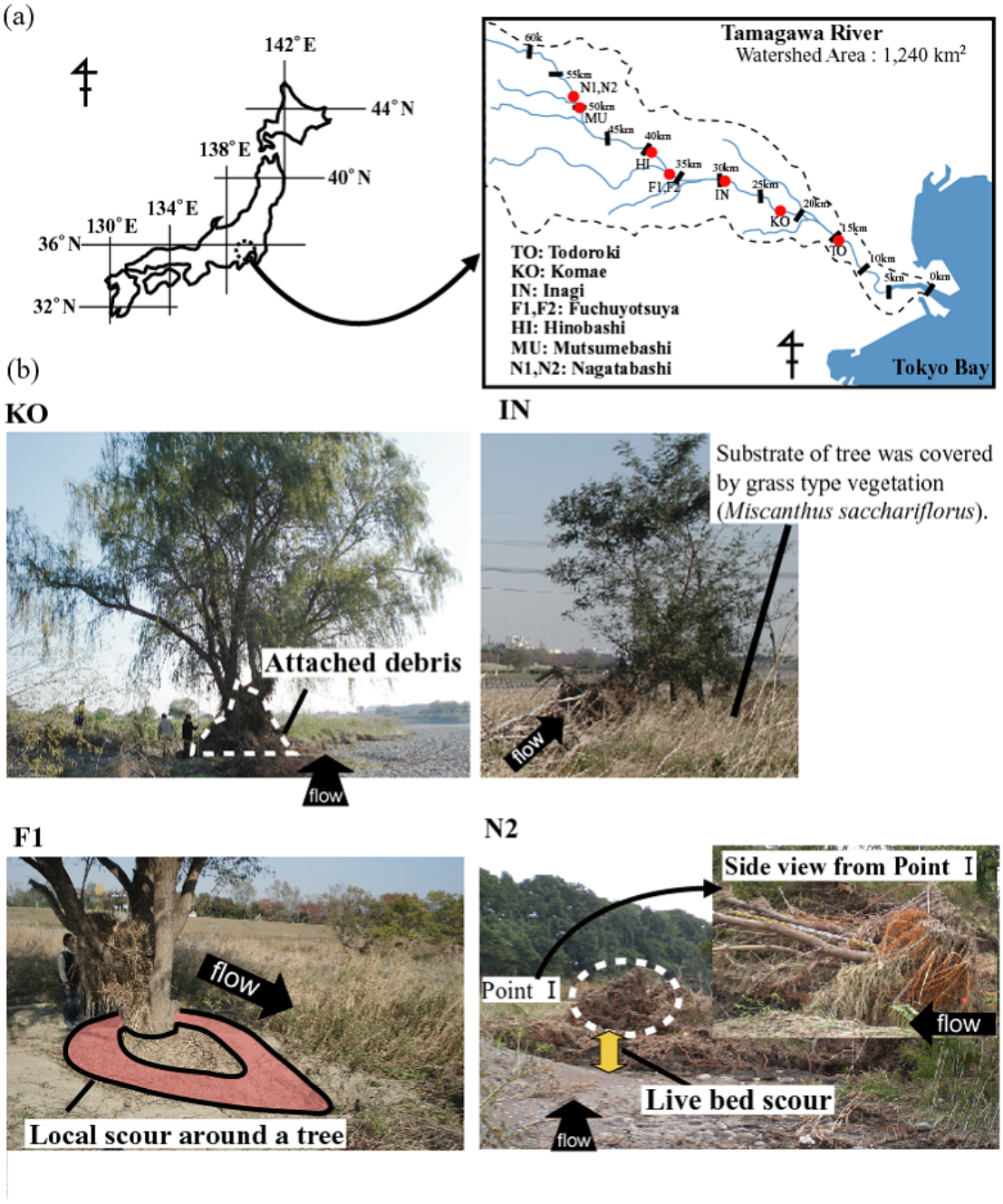
(a)
142°E
44°N
138°E
40°N
134°E
130°E
36°N
32°N
Tamagawa River
Watershed Area : 1,240 km²
60k
55km
N1,N2
50km
MU
45km
40km
HI
35km
F1,F2
30km
IN
25km
KO
20km
15km
TO
10km
5km
0km
TO: Todoroki
KO: Komae
IN: Inagi
F1,F2: Fuchuyotsuya
HI: Hinobashi
MU: Mutsumebashi
N1,N2: Nagatabashi
Tokyo Bay
(b)
KO
Attached debris
flow
IN
Substrate of tree was covered by grass type vegetation (Miscanthus sacchariflorus).
flow
F1
flow
Local scour around a tree
N2
Side view from Point I
Point I
flow
Live bed scour
flow

Fig. 4

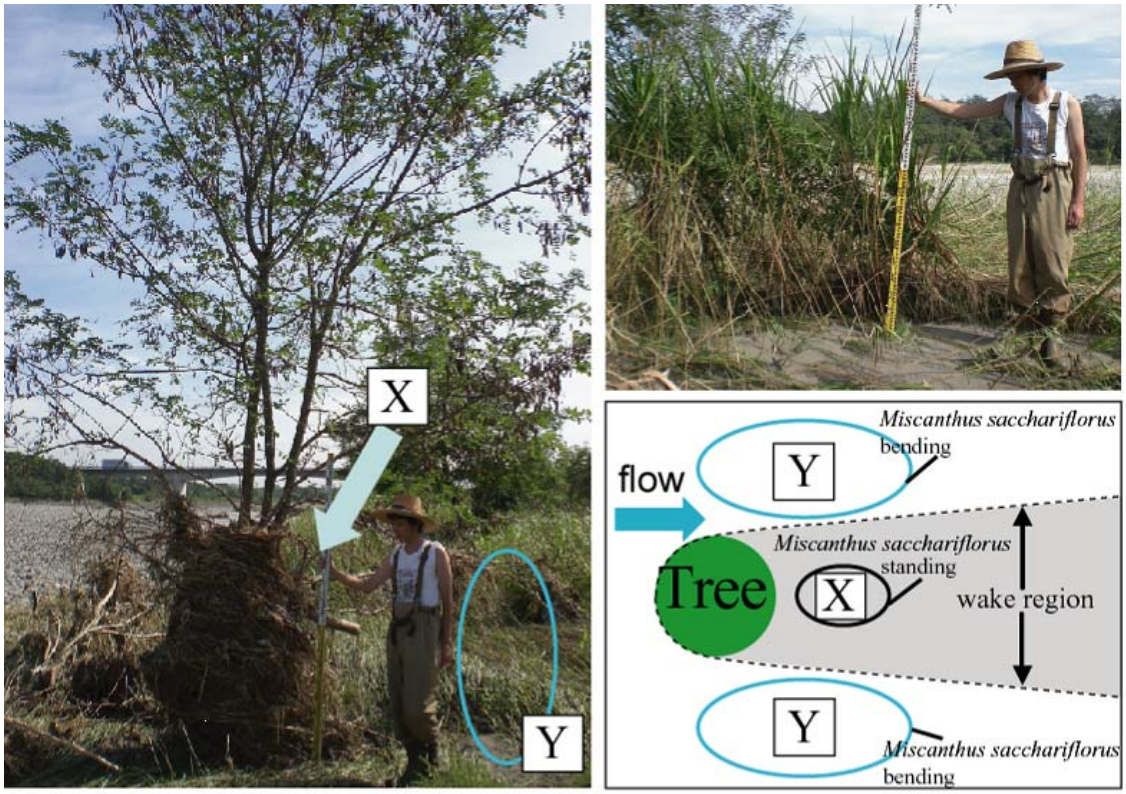
X
Y
Miscanthus sacchariflorus
bending
flow
Y
Miscanthus sacchariflorus
standing
Tree
X
wake region
Y
Miscanthus sacchariflorus
bending

(a)

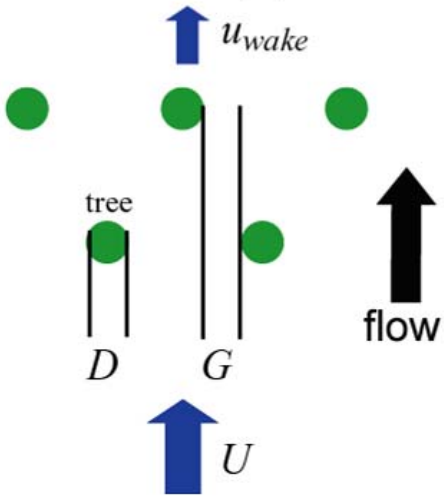
u_{wake}
tree
flow
D
G
U

(b)

Fig. 5

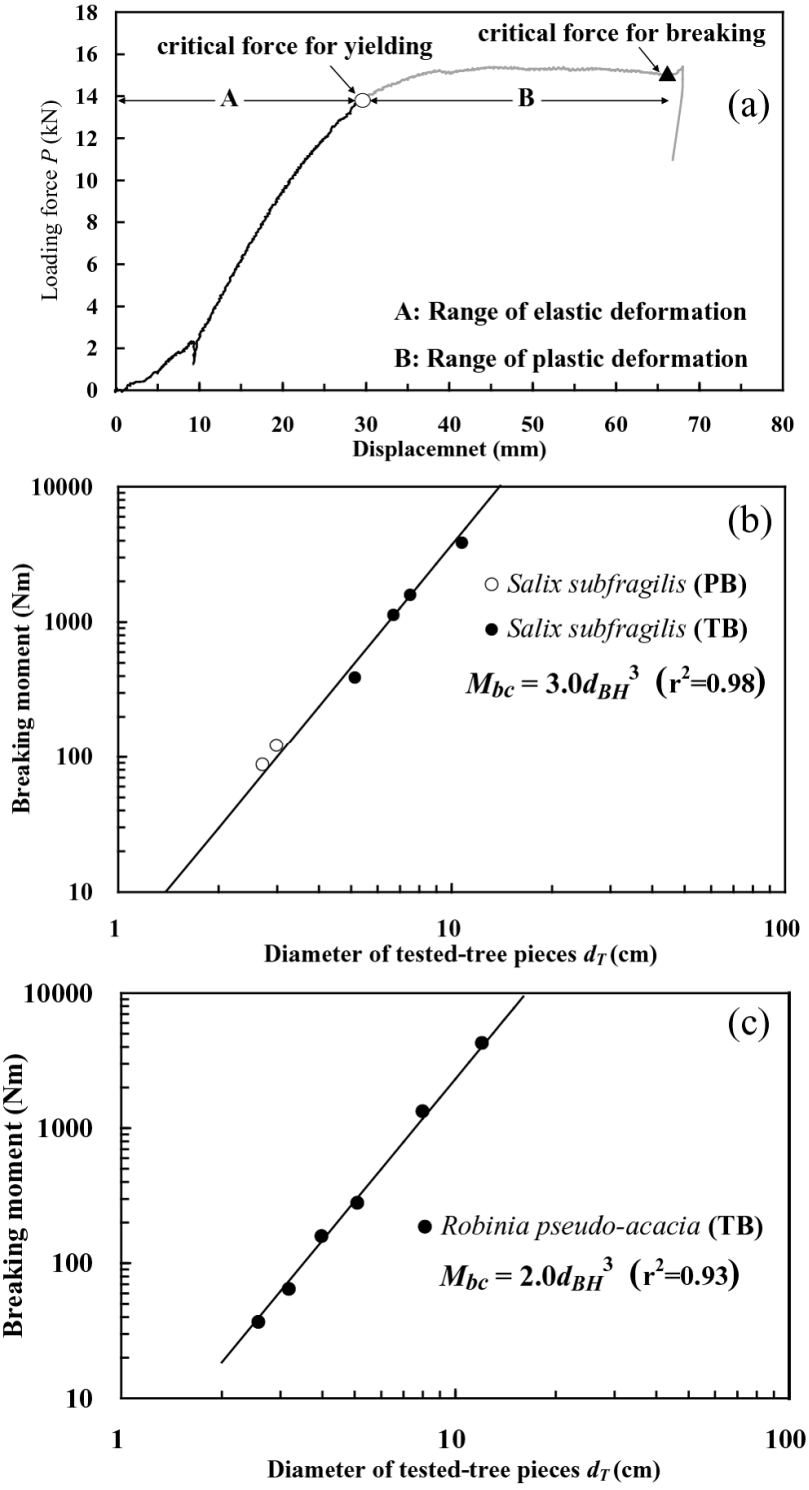
critical force for yielding
critical force for breaking
A
B
(a)
Loading force P (kN)
Displacemnet (mm)
A: Range of elastic deformation
B: Range of plastic deformation
(b)
Breaking moment (Nm)
Diameter of tested-tree pieces d_T (cm)
Salix subfragilis (PB)
Salix subfragilis (TB)
$M_{bc} = 3.0 d_{BH}^3$ (r^2=0.98)
(c)
Robinia pseudo-acacia (TB)
$M_{bc} = 2.0 d_{BH}^3$ (r^2=0.93)

Fig. 6

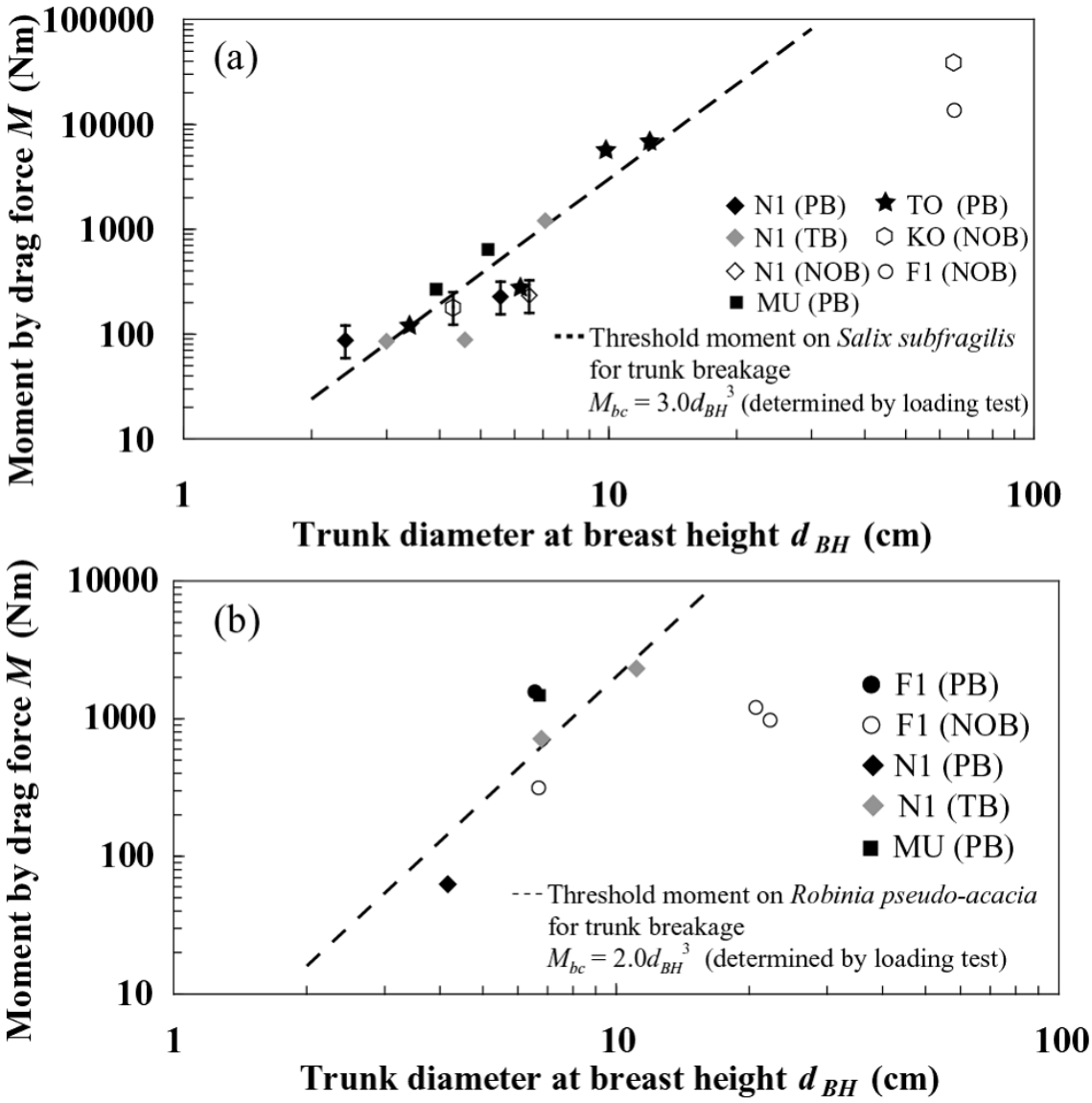
(a)
Moment by drag force M (Nm)
100000
10000
1000
100
10
1
10
100
Trunk diameter at breast height d_{BH} (cm)
N1 (PB)
TO (PB)
N1 (TB)
KO (NOB)
N1 (NOB)
F1 (NOB)
MU (PB)
Threshold moment on Salix subfragilis for trunk breakage
$M_{bc} = 3.0 d_{BH}^3$ (determined by loading test)
(b)
Moment by drag force M (Nm)
10000
1000
100
10
1
10
100
Trunk diameter at breast height d_{BH} (cm)
F1 (PB)
F1 (NOB)
N1 (PB)
N1 (TB)
MU (PB)
Threshold moment on Robinia pseudo-acacia for trunk breakage
$M_{bc} = 2.0 d_{BH}^3$ (determined by loading test)

Fig. 7

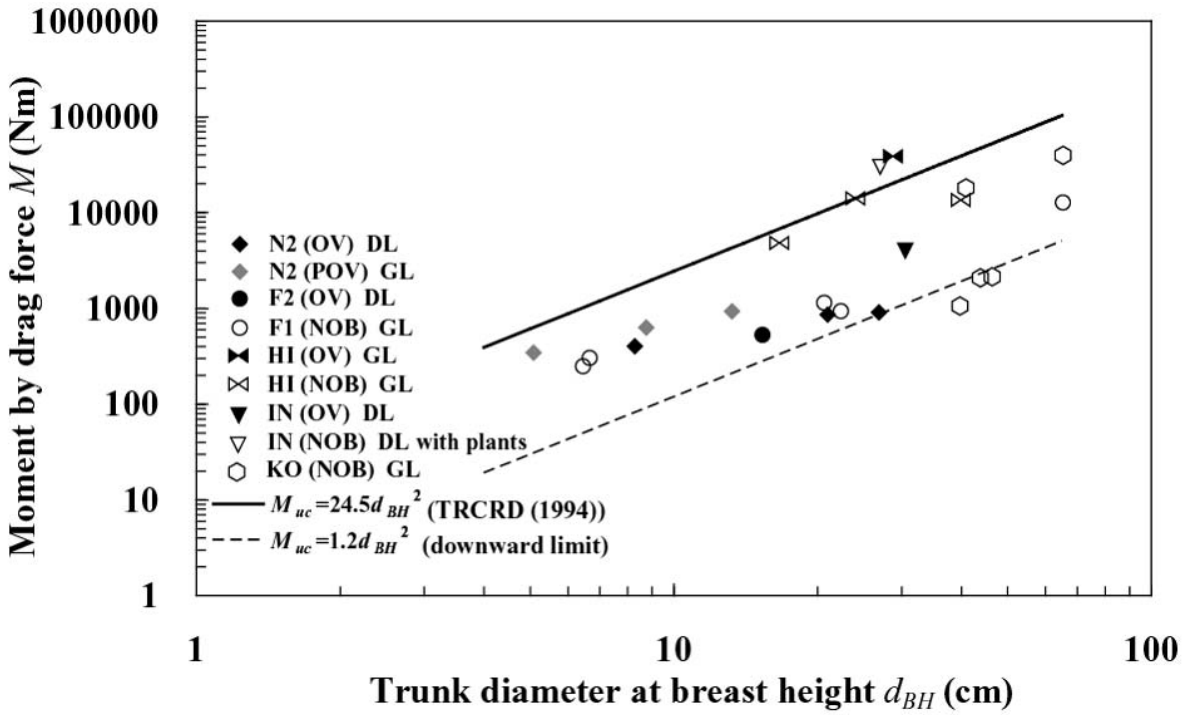
1000000
100000
10000
1000
100
10
1
Moment by drag force M (Nm)
N2 (OV) DL
N2 (POV) GL
F2 (OV) DL
F1 (NOB) GL
HI (OV) GL
HI (NOB) GL
IN (OV) DL
IN (NOB) DL with plants
KO (NOB) GL
M uc =24.5d BH 2 (TRCRD (1994))
M uc =1.2d BH 2 (downward limit)
1
10
100
Trunk diameter at breast height d BH (cm)

Fig. 8

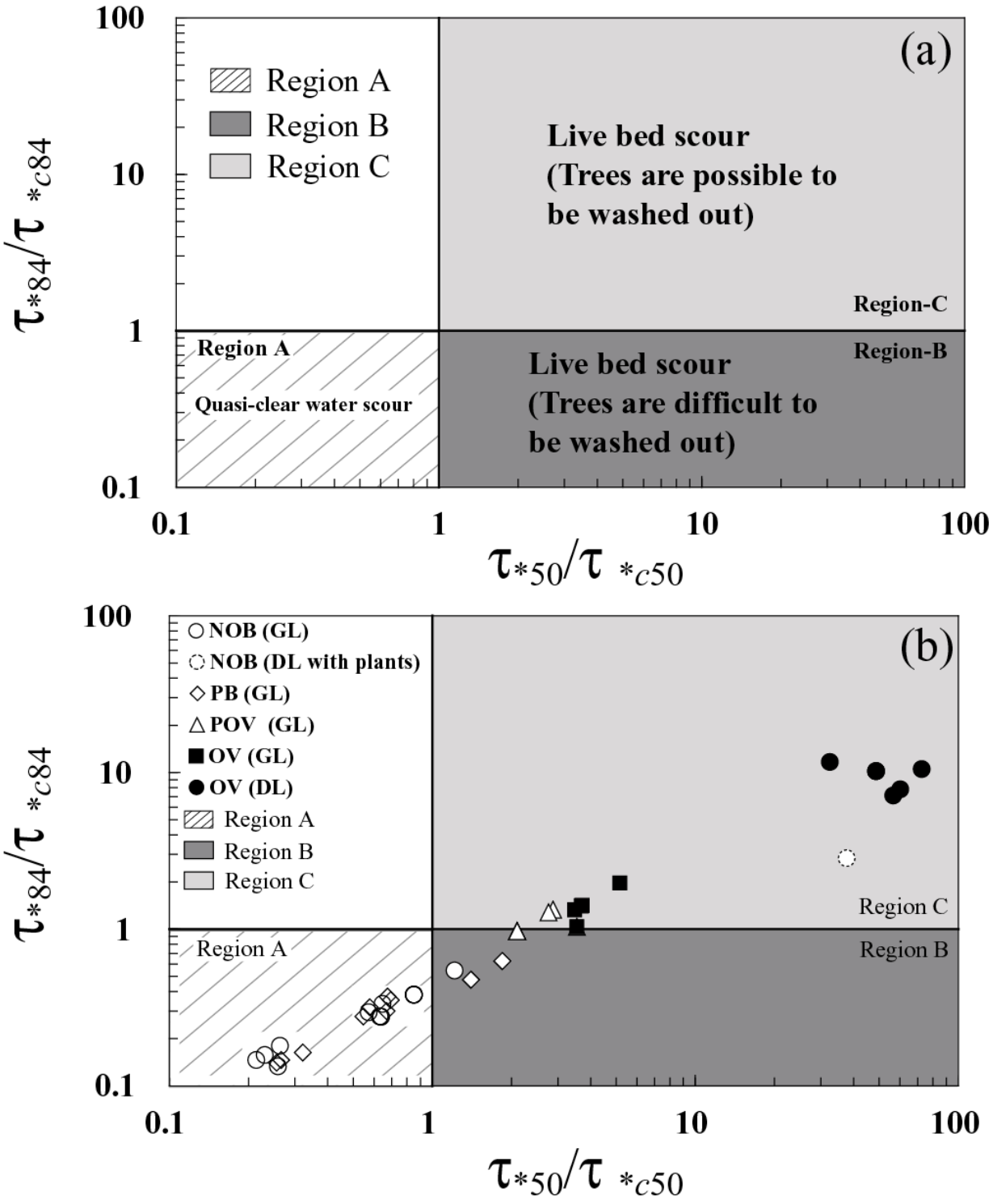
(a)
Region A
Region B
Region C
Live bed scour
(Trees are possible to
be washed out)
Region-C
Region A
Quasi-clear water scour
Region-B
Live bed scour
(Trees are difficult to
be washed out)
100
10
1
0.1
0.1
1
10
100
τ*84/τ *c84
τ*50/τ *c50
(b)
NOB (GL)
NOB (DL with plants)
PB (GL)
POV (GL)
OV (GL)
OV (DL)
Region A
Region B
Region C
Region C
Region A
Region B
100
10
1
0.1
0.1
1
10
100
τ*84/τ *c84
τ*50/τ *c50

Fig. 9

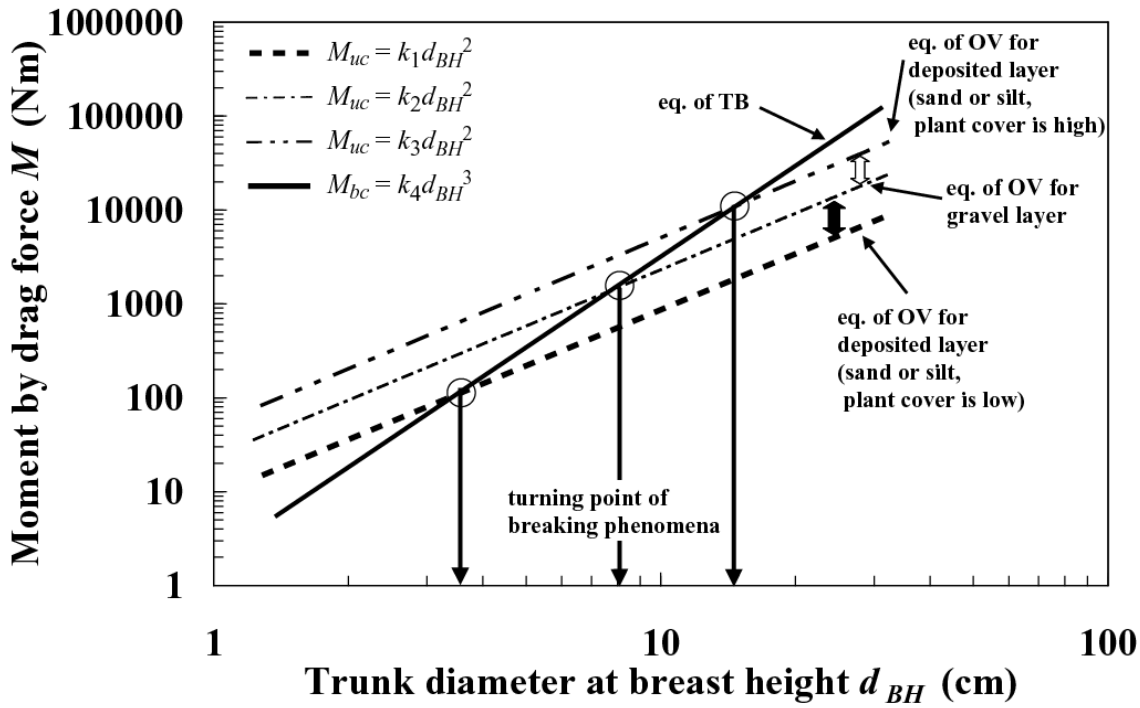
Moment by drag force M (Nm)
1000000
100000
10000
1000
100
10
1
$M_{uc} = k_1 d_{BH}^2$
$M_{uc} = k_2 d_{BH}^2$
$M_{uc} = k_3 d_{BH}^2$
$M_{bc} = k_4 d_{BH}^3$
eq. of TB
eq. of OV for deposited layer (sand or silt, plant cover is high)
eq. of OV for gravel layer
eq. of OV for deposited layer (sand or silt, plant cover is low)
turning point of breaking phenomena
1
10
100
Trunk diameter at breast height d_{BH} (cm)

(a)

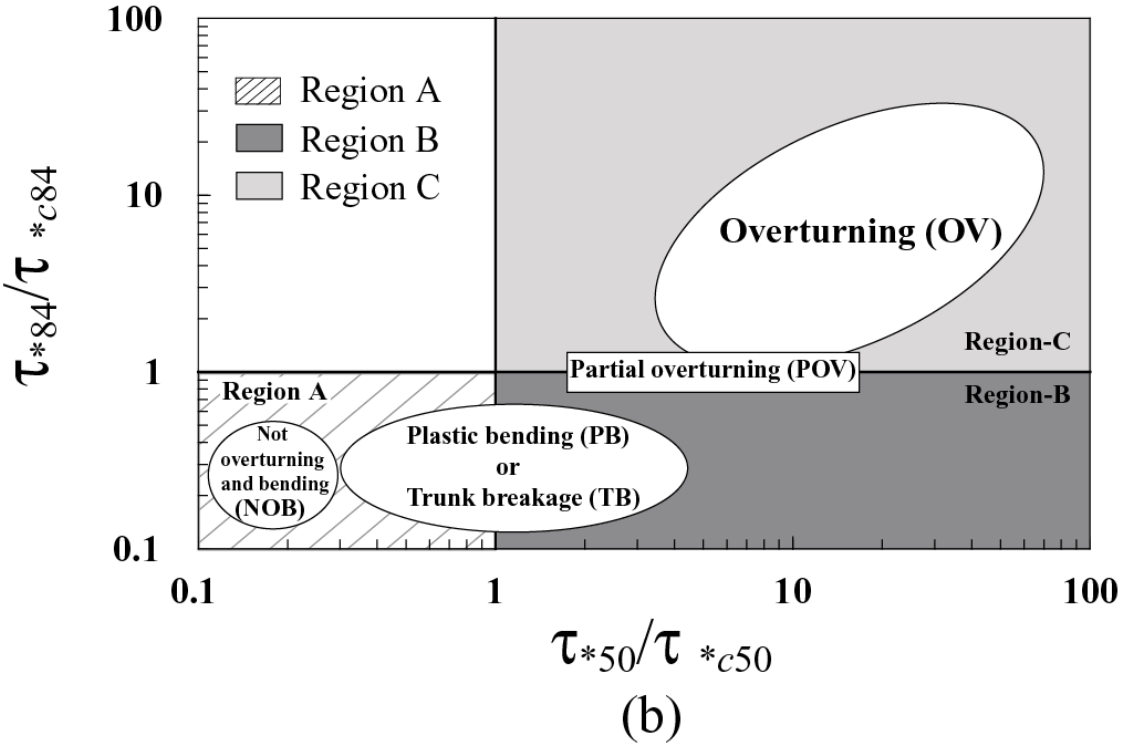
τ_{*84}/τ_{*c84}
100
10
1
0.1
Region A
Region B
Region C
Overturning (OV)
Region-C
Partial overturning (POV)
Region-B
Region A
Not overturning and bending (NOB)
Plastic bending (PB) or Trunk breakage (TB)
0.1
1
10
100
τ_{*50}/τ_{*c50}

(b)

Fig.10

Table 1 Locations and flood characteristics of tree-damaged sites

Notation	Location	Latitude	Longitude	Riverbed gradient	Water depth at Typhoon 9 event (m)**	Particle diameter (cm) d_{50}*	Particle diameter (cm) d_{84}*
TO	Todoroki	35°35'25"N	139°39'18"E	1/739	1.6 - 4.2	6.0-10.8	12.9 - 16.8
KO	Komae	35°37'15"N	139°34'53"E	1/739	1.3 - 3.5	7.4 - 8.3	11.3 - 12.1
IN	Inagi	35°39'06"N	139°29'56"E	1/512	3.0 - 3.2	0.1 - 0.2	0.4 - 1.1
F1	Fuchuyotsuya (upstream)	35°39'31"N	139°26'27"E	1/297	1.4 - 1.7	4.8-6.5	7.6 - 9.5
F2	Fuchuyotsuya (downstream)	35°39'25"N	139°26'37"E	1/297	1.4 - 2.0	0.2 - 0.3	0.4 - 0.7
HI	Hinobashi	35°40'55"N	139°24'50"E	1/290	2.0 - 2.5	11.0 - 12.0	20.1 - 20.8
MU	Mutsumebashi	35°42'45"N	139°19'50"E	1/228	1.1 - 2.3	8.9-16.9	15.7 - 25.4
N1	Nagatabashi (upstream)	35°44'21"N	139°19'05"E	1/228	1.9 - 2.5	4.0 - 6.0	6.9 - 12.9
N2	Nagatabashi (downstream)	35°44'19"N	139°19'06"E	1/228	1.9 - 2.6	0.2 - 0.5	0.6-0.8

* d_{50} and d_{84} are grain sizes at which 50% and 84%, respectively, of the material weight is finer.

** The water depth was assumed by the height of flood water marks on the investigated trees